ChemPhysMater 3 (2024) 24–35

Contents lists available at ScienceDirect

ChemPhysMater

journal homepage: https://www.keaipublishing.com/en/journals/chemphysmater/

Review Article

In-situ observation of structural evolution of single-atom catalysts: From synthesis to catalysis

Lei Wang [a,*], Shuyuan Lyu [b], Shuohao Li [c,*]

[a] School of Chemistry and Chemical Engineering, Yangzhou University, Yangzhou 225009, China
[b] School of Art and Design, Huaiyin Institute of Technology, Huaian 223003, China
[c] School of Safety Engineering, China University of Mining and Technology, Xuzhou 221116, China

ARTICLE INFO

Keywords:
Single-atom catalysts
Structural transformation
Atomization
Environmental electron microscope

ABSTRACT

Atomically dispersed single-atom catalysts (SACs) have been extensively studied over the past decade because of their high atom utilization efficiencies and specific selectivities. Although numerous strategies have been proposed to obtain SACs with high densities and stabilities, the transformation mechanism that occurs during the reaction is still unclear. This review summarizes the structural evolution of SACs in the preparation process and reaction with various electron microscopy techniques at atomic scale under environmental conditions. Current state-of-the-art environmental electron microscopy studies on SACs mainly focus on porous carbons, metals or metal oxides, and some specific composite materials. The dynamic evolution of SACs under various reaction conditions is also investigated in this study. Finally, we highlight the challenges and drawbacks of the current studies and the prospects for the future exploration of SACs with environmental strategies.

1. Introduction

Supported heterogeneous metal catalysts are widely used for the production of the majority of chemicals, materials, and energy in modern society because of their stability and ease of separation [1,2]. In contrast, their low atom-utilization efficiency and the complicated systems (e.g., size, structure, defects) result in low activity and selectivity. In addition, it is challenging to elucidate a clear relationship between the structure and reactivity in these complex systems. These issues may be addressed by using atomically dispersed single-atom catalysts (SACs) with specific active sites and almost 100% atom utilization efficiency [3]. Numerous reports have featured SACs since "single-atom catalysis" was pioneered by Zhang in 2011 [4], and SACs have been the focus of research in the past decade [5–9]. The SACs displayed unexpected activity and high specific selectivity compared with their counterpart metal particles.

A single metal atom does not actually exist on the surface of a specific support owing to its high surface free energy [3], these isolated metal atoms are generally fixed on the carrier by coordinating with their neighboring atoms. The microenvironment of a single site in SACs is similar to that of a molecular complex during the catalytic process, thereby endowing this new type of heterogeneous catalyst with homogeneous properties, such as superior activity and specific selectivity. Therefore, SACs are ideal candidates for bridging homogeneous and heterogeneous catalytic reactions [10]. SACs display excellent activity and selectivity in various heterogeneous thermocatalytic processes, such as hydrogenation/dehydrogenation [6,11–13], CO oxidation [4,8,14], and water-gas shift [15,16]. Moreover, they demonstrate remarkable electrocatalytic activity for several reactions, including N_2 nitrogen reduction reaction [17], oxygen reduction reaction [18,19], formic acid oxidation reaction [20], CO_2 reduction reaction [21], and hydrogen evolution reaction [22]. In addition, SACs have promising applications in biomedical fields [23], owing to their high atom utilization efficiency and the presence of specific active sites. The geometric or electronic active sites of SACs can be flexibly regulated by supporting metals on various carriers, such as porous carbons or carbon-based materials [24], carbides [25], zeolites [26], metals or metal oxides [6,27,28], and sulfides [29]. In addition, numerous strategies have been proposed to fabricate high performing SACs, such as conventional wet-impregnation [24] co-precipitation [4,30], atomic layer deposition [14,31], pyrolysis [32–34], photochemical strategies [6], ice photochemical reduction methods [35], and thermal emission strategies [36,37]. More encouragingly, atomically dispersed dual-atom pairs or bimetallic dimers can provide a synergistic effect on the catalytic process, and might be a new method for regulating the catalysis [38–40].

Many high-end characterization techniques and strategies have been proposed to aid the understanding of the active centers of SACs, including electron microscopy, X-ray absorption spectroscopy (XAS),

* Corresponding authors.
E-mail addresses: leiwang88@yzu.edu.cn (L. Wang), shuohaoli@cumt.edu.cn (S. Li).

https://doi.org/10.1016/j.chphma.2023.03.003
Received 20 January 2023; Received in revised form 21 March 2023; Accepted 23 March 2023
Available online 7 April 2023

X-ray photoelectron spectroscopy (XPS), and Fourier-transform infrared (FTIR) spectroscopy. Electron microscopy can provide directly observable results for a single atom or a small region of the catalyst supported on a solid support. For example, atomic resolution high-angle annular dark-field scanning transmission electron microscopy (HAADF-STEM) can distinguish between light and heavy elements, owing to the different Z-contrasts in the dark field [3,41]. Moreover, HRTEM can be used to identify the structural morphology of a single site [42,43]. Furthermore, atomic resolution electron energy-loss spectroscopy (EELS) can identify the valence states and isolated structures of single metals [44,45]. Both XPS and X-ray absorption near-edge spectroscopy can yield macrocosmic information about the electronic states of the catalysts. The coordination environment of SACs can be identified by fitting X-ray absorption near-edge spectroscopy and extended X-ray absorption fine structures [46–48]. FTIR can confirm the interaction between the adsorbent molecules and metal surface. The structure and configuration of the active sites can be identified by the adsorption of specific probe molecules. For example, a Pt-based catalyst was found to be a single Pt atom catalyst using CO as a probe molecule during IR spectroscopy [4]. Due to the particularity of a single site, the peak position of the CO molecule that was adsorbed on a single Pt atom was different from that adsorbed on nanoparticles [49]. In addition, the IR extinction coefficient ratio of CO molecules adsorbed on single Pt atoms and nanoparticles can be obtained by combining temperature-programmed oxidation and mass spectrometry to quantify the CO adsorption sites. For example, single-atom Pt catalysts exhibit only signals for linearly bonded CO, whereas Pt clusters exhibit signals for both linear and bridged adsorbed CO. The dynamic evolution of the surface structure and activity at the atomic scale during the reaction can provide direct and powerful evidence of the reaction mechanism [45,50,51]. Although there have been some reports on the dynamic changes in metal nanoparticles under environmental conditions, reviews on the dynamic structural evolution of single-atom sites are rare [52–55]. Some research groups have studied the transformation of metal particles into single atoms using environmental TEM because of the rapid development of in-situ techniques and facilities [56–58]. In this review, we summarize recent in-situ studies on SACs under various reaction conditions over different carriers (Fig. 1). We believe that evidence obtained from direct observations in situ will provide a deeper understanding of the reaction mechanism. Finally, we conclude by discussing the challenges and prospects for the in-situ study of SACs under environmental conditions.

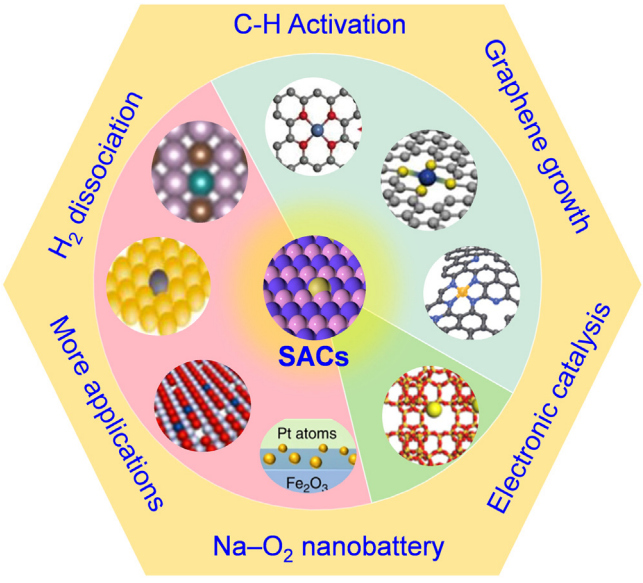

Fig. 1. Schematic diagram of in-situ observation of structural evolution of SACs over various carriers under different reaction conditions.

2. Transformation of SACs over different substrates

SACs can be synthesized on numerous carriers, including metals or metal oxides [5,28,59,60], porous carbons [24,56,61,62], carbides [25,63], sulfides [29], nitrides [39,64], and zeolites [65]. Most of these materials are good substrates for the in-situ observation of the structural evolution of various metals.

Most of these studies focused on the transformation of nanoparticles into single atoms under high-temperature conditions. Conventionally, metal nanoparticles undergo serious Ostwald ripening under high-temperature treatment [41,66–68],which severely hampers the application of heterogeneous catalysts [69,70]. The sinter-resistant SACs show immense potential in the chemical engineering industry. In addition, the volatilization and trapping of single atoms over a reducible carrier system can promote the large-scale manufacturing of SACs.

2.1. Metal oxides

Datye reported that Pt particles emit PtO_2 species under oxidizing conditions and are trapped by other metal oxides to form stable active single sites [5,71]. The strategy of trapping of atoms on metal oxides, induced by strong metal-support interactions, can be applied to prepare various SACs. Pt atoms tend to occupy the step edges of a ceria carrier; thus, ceria with polyhedral and nanorod structures stabilizes the Pt atoms more effectively than cubic ceria. Recently, Qiao et al. successfully synthesized single-atom Pt catalysts over an Fe_2O_3 carrier using the same method, and significantly improved the Pt loading from 0.17 wt% to 0.3 wt% [4,72]. The research team directly observed the structural evolution process of the Fe_2O_3 supported Pt particles at 800 ˚C under a flow of 1 bar O_2 using in-situ HAADF-STEM. Approximately 300 Pt particles with an average size of approximately 3 nm were observed (Fig. 2(a)). The number of Pt particles decreased to ~200 after annealing for 1200 s at 800 ˚C. Some Pt particles (particle sizes of 2–3 nm) shrank and/or disappeared during the high-temperature treatment process, while larger particles (~10 nm) retained their original structure. The smaller the particle size, the faster the Pt particles disappear. For example, the smaller Pt particles (e.g., particle 1, Fig. 2) disappeared in 35 s, whereas the larger Pt particles required 45 s to disintegrate.

The atomization process of metal particles at high temperatures is different from that of conventional Ostwald ripening, and exhibits strong sinter-resistance. However, a single-atom Pt catalyst could not be obtained in an inert Ar atmosphere; instead, reducible Fe_2O_3 with a non-reducible Al_2O_3 support was used, and severe aggregation of the Pt particles was observed. In other words, single-atom Pt catalysts could only form in an oxidizing atmosphere over reducible carriers (Figs. 2(b)(c)).

Theoretical calculations demonstrated that the release of PtO_2 species at 800 ˚C under an oxidizing atmosphere was approximately −0.61 eV per PtO_2 (Fig. 2(d)). However, the evaporation energy of a single Pt atom under an inert environment at the same temperature was 4.00 eV, indicating that the preparation of SACs was impractical under inert or reducible gas atmospheres at high temperatures [72]. In addition, the binding of the PtO_2 species via a four-fold distorted square configuration over the reducible Fe_2O_3 surface is highly exothermic at 800 ˚C. However, it is difficult to form stable Pt-O bonds on alumina surfaces because of the irreducibility of Al^{3+} [72]. The experimental and calculated results indicated that SACs are more easily synthesized on reducible carriers in an oxidizing environment. The authors subsequently observed the structural evolution of Ru particles with in-situ HAADF-STEM by physically mixing RuO_2 powders with the Fe-substituted $MgAl_2O_4$ ($MgAl_{1.2}Fe_{0.8}O_4$) support [73]. The RuO_2 nanoparticles on $MgAl_{1.2}Fe_{0.8}O_4$ also shrank at high temperatures in an O_2 environment, indicating the volatilization of RuO_2 to form atomic Ru catalysts. Experimental and theoretical calculations demonstrated that the presence of Fe atoms strengthened the metal-support interaction and weakened the Ru–Ru interaction, which promoted the disper-

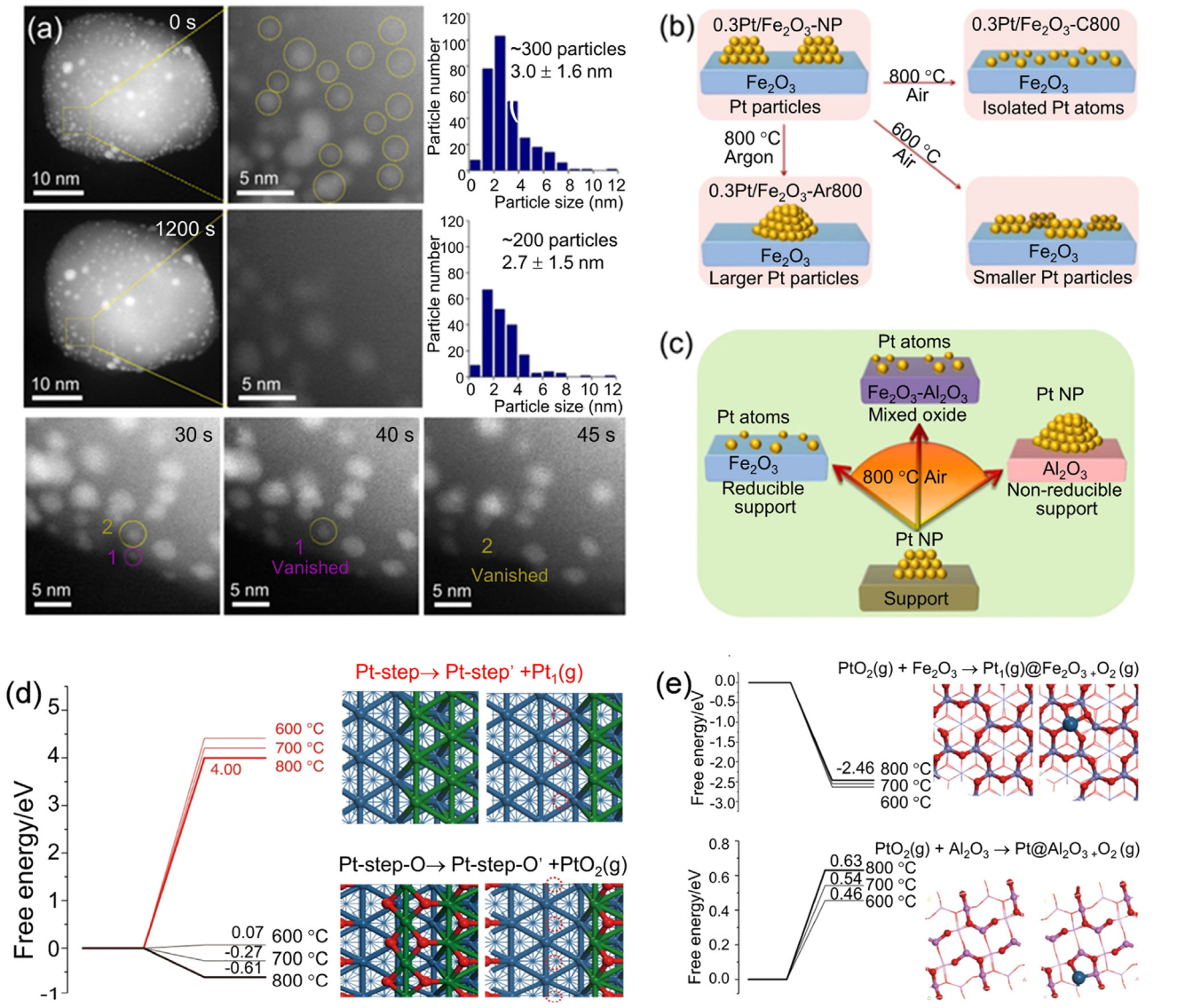

Fig. 2. Transformation of Pt nanoparticles to single atoms over metal oxides. (a) In-situ observation of Fe_2O_3 supported Pt nanoparticle structure evolution annealed at 800 ˚C in 1 bar O_2. (b) Schematic illustration of Fe_2O_3 supported Pt nanoparticle transformation under different atmospheres. (c) Schematic illustration of Pt nanoparticle structure evolution supported on different carriers annealed in air. (d) Calculated energies for evaporation of Pt atom and PtO_2 unit from Pt (221) step. (e) Optimized structures and free energy profiles of PtO_2 anchoring on Fe_2O_3 (0001) and Al_2O_3 (010) surfaces.

sion of RuO_2. This strategy allows for a successful scalable production of SACs (1 kg scale).

Wang prepared noble Ag SACs on MnO_2 carriers using a similar synthetic strategy [21]. The results indicated that the driving force for the preparation of atomic Ag catalysts was the reconstruction of the MnO_2 (211) lattice plane into the (310) lattice plane under high thermal treatment; this was confirmed by in-situ TEM and in-situ X-ray diffraction (XRD).

2.2. Carbon-based materials

Similar to reducible metal oxide supports, metals can also be anchored on carbon-based materials by coordinating with carbon or doped heteroatoms during the high-temperature treatment process [33,74–76]. The pyrolysis of metal-N_x macrocycles/composites or metal-organic frameworks (MOFs) at high temperatures exhibits excellent potential for the preparation of carbon-supported SACs [33,77–79]. MOFs are a perfect class of materials for fabricating SACs by optimally configuring a stable coordination environment. Specifically, zeolitic imidazolate frameworks (ZIFs) have been extensively studied among the MOFs [58,62,74,80–85]. Pyrolysis is generally conducted in an inert atmosphere because carbon-based materials cannot withstand high temperatures in an oxidizing atmosphere. During pyrolysis, the organic linkers of the MOFs are transformed into N-doped carbon carriers, and the metal nodes are reduced by carbon at high temperatures. The Zn atoms serve the purpose of isolation, and the evaporation of Zn generates a stable anchor site in situ that can coordinate with the target metals during pyrolysis [61]. Although there are numerous reports on the pyrolysis of ZIFs to prepare SACs, the exact evolution of the structure and formation mechanism have seldom been reported.

Li et al. directly observed the transformation of noble metal nanoparticles into thermally stable single atoms over ZIF-derived carbon at high temperatures in inert Ar (Fig. 3(a)) [56]. The particle size of Pd metals increased, while the number of Pd particles decreased during the temperature change from 100 to 900 ˚C, demonstrating that agglomeration and atomization coexisted. The Ostwald ripening and atomization process accelerated upon increasing the temperature to 1000 ˚C, and the Pd particles disappeared eventually, demonstrating that the atomiza-

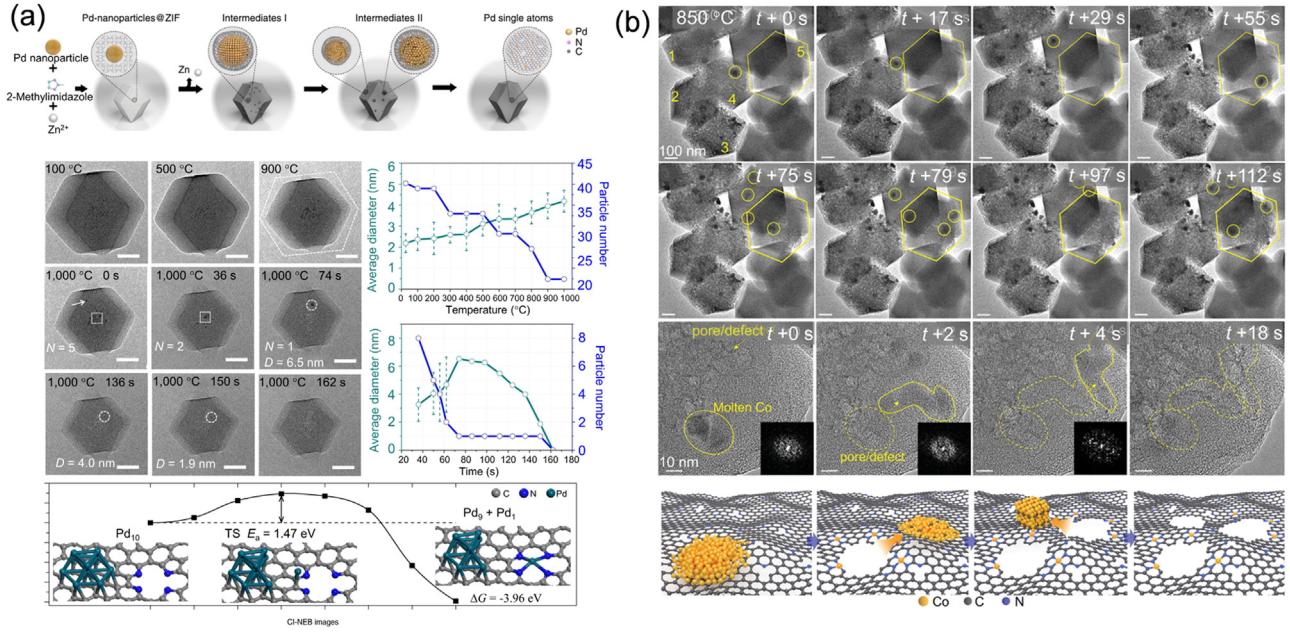

Fig. 3. (a) Schematic illustration and TEM images of the transformation of noble Pd metal nanoparticles to single atoms over ZIF-derived carbon materials. *N* and *D* are the number and average diameter of Pd particles, respectively. Scale bar: 50 nm. (b) Time-sequenced TEM images and schematic illustration of non-noble Co etching of ZIF-derived carbon.

tion process was dominant. The bonding strengths of Pd-N and Pd-Pd determined the atomization or agglomeration process. Theoretical calculations revealed that Pd coordinated with two pyrrolic N atoms and two pyridinic N atoms presented a very stable configuration (Fig. 3(a)), which could have determined the atomization process. However, significant metal sintering was observed upon replacing the carrier with traditional carbon under the same conditions. This versatile top-down method can be used for the synthesis of single Pd, Pt, and Au catalysts [56]. Recently, Zheng et al. studied the transformation of non-noble Co metals via the pyrolysis of a Co/Zn-ZIF material. Similar to the noble metals, the Co metals also underwent agglomeration and atomization during the high-temperature treatment process and finally formed

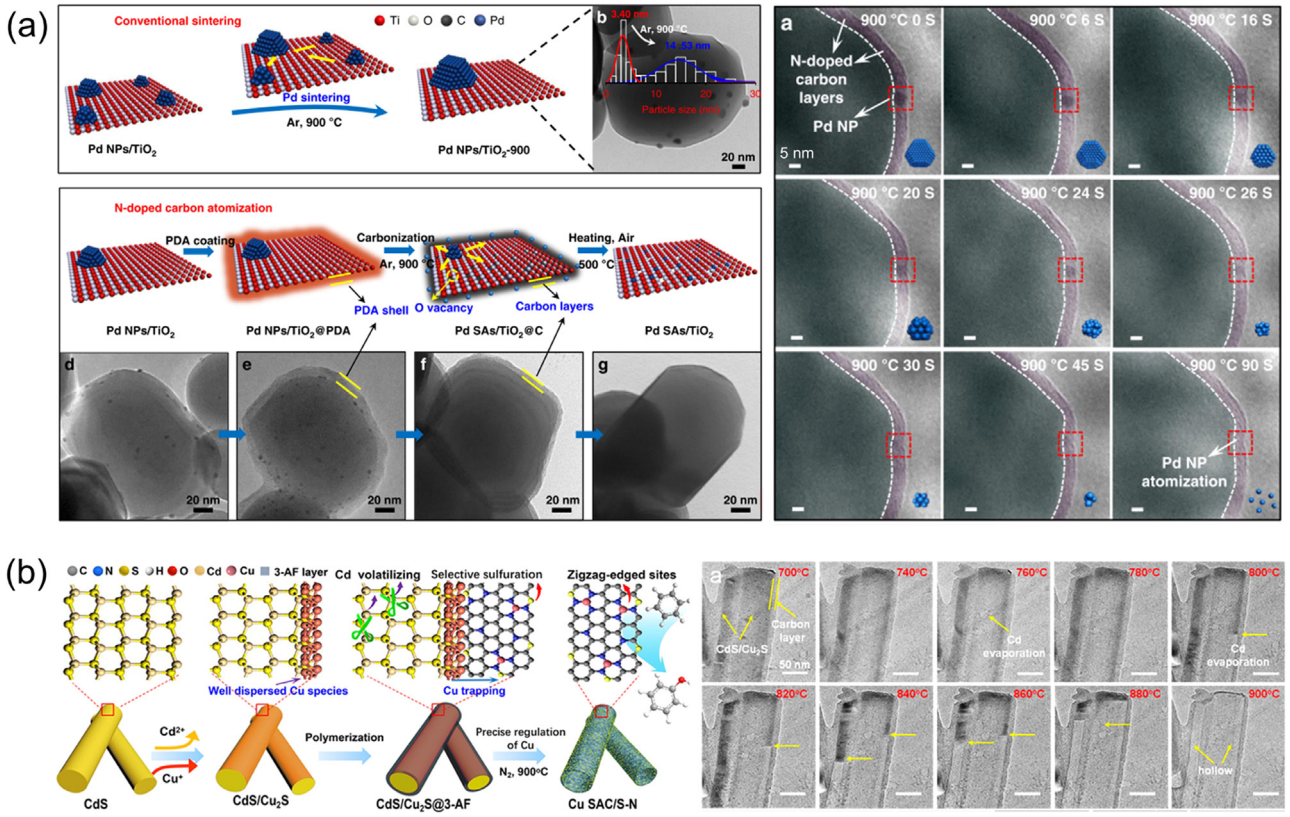

Fig. 4. Transformation of metal nanoparticles into single atoms over (a) carbon modified TiO_2 and (b) sulfide composites.

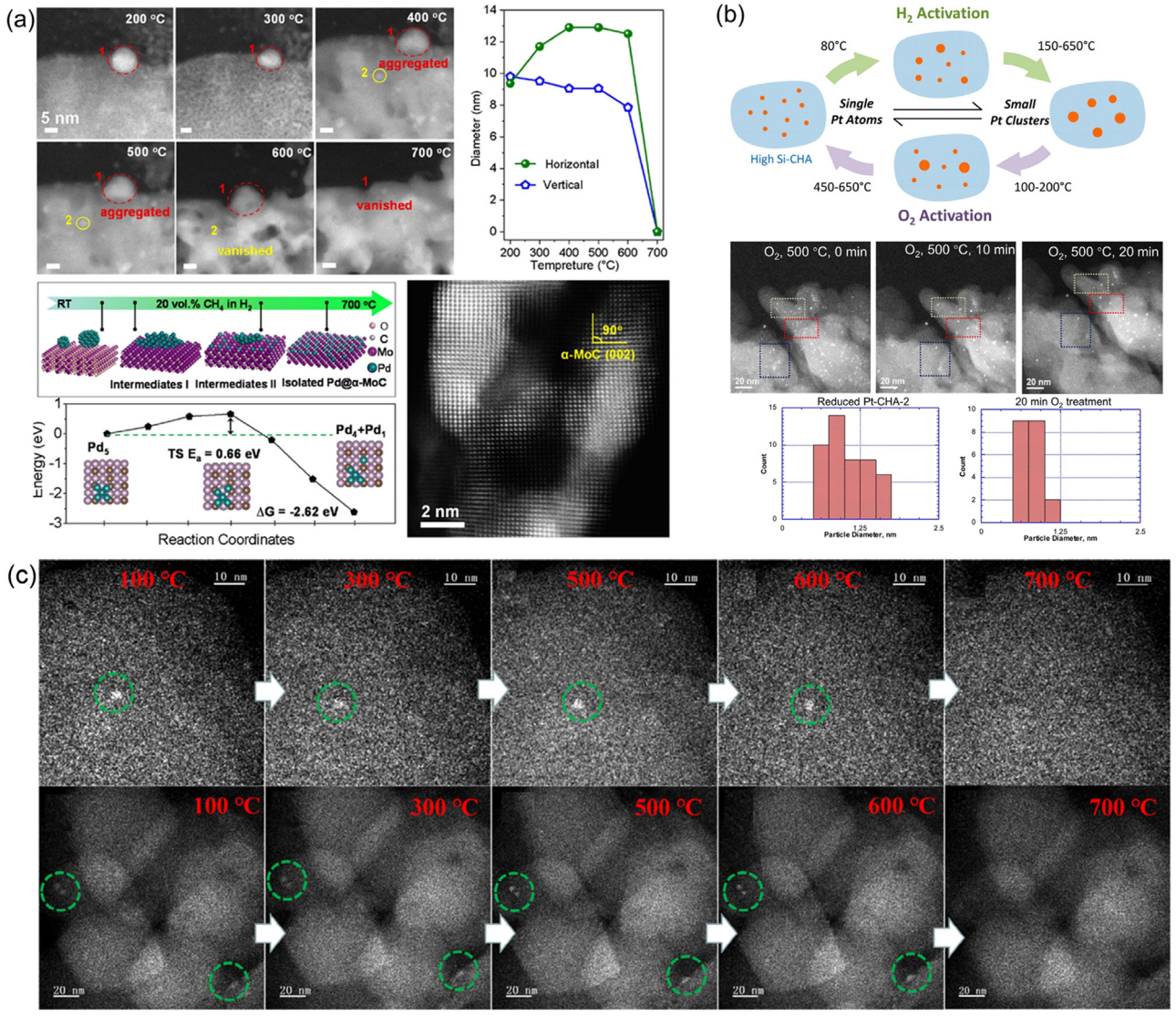

Fig. 5. Transformation of metal nanoparticles into single atoms over (a) α-MoC, (b) high-silica chabazite zeolite, and (c) ZSM-5.

single-atom Co catalysts [58]. The researchers concluded that the formation of single-atom Co catalysts can occur in four stages. The Co species were reduced and aggregated into metallic Co clusters via the pyrolysis of ZIF at a relatively low temperature (500 °C). The ultrafine Co clusters were stable and well-dispersed at a much higher temperature (800 °C). However, at 850 °C, Co agglomerated into nanoparticles and the molten Co droplets moved and etched the ZIF-derived carbon to generate a porous structure (Fig. 3(b)). At this stage, carbon dissolved into the Co nanoparticles to form carbides. Finally, the cobalt carbide nanoparticles sublimated or evaporated and anchored on the N-doped porous carbon at 1000 °C.

Atomization and trapping using nitrogen anchor sites can generally be applied to functional carbon-modified composite materials [86–88]. Wu deposited polydopamine (PDA) on a Pd/TiO_2 surface to form a core-shell structure; the PDA was carbonized to nitrogen-doped carbon with abundant nitrogen defects at high temperatures (Fig. 4(a)) [86]. The in-situ observations indicated that the nitrogen defects provided diffusion and anchoring sites for the mobile metal species that detached from the particles. More importantly, the loss of catalytic activity due to severe sintering could be recovered through this atomization process [86]. In addition to the nitrogen defect anchoring sites, Wu developed an edge-rich S and N dual defect material with CdS nanorods; the dual anchoring sites played a significant role in the atomization of various metals (Fig. 4(b)) [87].

Conventionally, catalysts are prone to poisoning by sulfur species; however, sulfide- and sulfur-doped carbon material-supported SACs exhibit superior catalytic performances toward various reactions, including benzene oxidation [87], CO_2 hydrogenation [29], and electrocatalysis [19,24].

2.3. Other supports

Liu and Wang directly observed the transformation of Pd crystals into single-atom Pd catalysts over an α-MoC substrate, which was derived from the carbonization of MoO_3, under atmospheric pressure (20 vol.% CH_4/H_2) [89]. MoO_3 retained their initial structures at low temperature ($\leq$ 300 °C), while the MoO_3 carrier support collapsed and formed an open-framework structure upon increasing the temperature to 400 and 500 °C (Fig. 5(a)). The in-situ XRD revealed that the MoO_3 structure underwent the following transformation: MoO_x (200 °C), MoO_xC_y (350 °C), and α-MoC (> 650 °C). The Pd crystals started to aggregate between 300–500 °C and subsequently atomized at much higher temperatures (600–700 °C). Theoretical calculations demonstrated that the atomization of small Pd clusters (Pd_5) on the vacancy enriched α-MoC was ther-

modynamically and kinetically favorable (Fig. 5(a)). Studies have concluded that α-MoC is a perfect substrate for supporting various SACs that exhibit superior catalytic performance in chemoselective hydrogenation [90,91] and hydrogen production [44,92,93]. In-situ TEM results indicated that the transformation of Pt particles to single atoms over zeolites could be effective at temperatures < 700 ˚C [94,95]. Corma discovered the reversible transformation of single-atom Pt and ~1 nm clusters over a high-silica chabazite zeolite in O_2 and H_2 environments, respectively (Fig. 5(b)) [94]. Yu observed the atomization of Pt nanoparticles on ZSM-5 by increasing the temperature to 700 ˚C in an O_2 atmosphere (Fig. 5(c)) [95]. Calculations revealed that the Al atoms in zeolites provided anchoring sites to bind the PtO species, and the binding energy decreased with increasing calcination temperature.

As discussed above, the competition between the agglomeration and atomization processes plays a significant role in the formation of thermally stable SACs. Strong chemical metal-support interactions play a key role in ensuring atomization by anchoring atomically dispersed metal atoms. In addition, constructing specific structures and introducing defects or various heteroatoms into the substrates may be effective strategies for synthesizing SACs by forming an optimum configuration.

3. Reaction behavior of SACs

In-situ/operando observation of the behavior or structural evolution of the surface at the atomic scale could provide powerful and fundamental evidence for elucidating the structure-activity/selectivity relationships under the reaction conditions. Nevertheless, the inhomogeneity of the active sites remains the main obstacle in reliably resolving the reaction mechanisms. SACs with single or homogeneous active sites appear to be perfect candidates for bridging heterogeneous and homogeneous catalysis. Although there are numerous reports on the dynamic structural evolution of heterogenous catalysts with TEM or STEM under environmental conditions, reports describing the behavior of SACs under catalytic reaction conditions are rare [51,54,96–98]. It is still a challenge to observe single-site active sites under bright fields. In this section, we introduce studies on the dynamic evolution of SACs under catalytic reaction conditions.

3.1. Single-atom Au for catalyzing methane pyrolysis

Luo studied the structural evolution of nanoporous Au (NPG) for catalyzing methane pyrolysis using in-situ TEM with spatial resolution [99]. The thickness of the amorphous carbon increased during CH_4 pyrolysis, whereas an obvious decrease in the thickness of the NPG ligaments was observed during the catalytic process (Fig. 6(a)). The decrease in the Au surface area implied that numerous single Au atoms were released from the ligaments and then were dispersed or anchored onto the carbon layers. The abundant nanopores, including mesopores (3–7 nm) and micropores (~0.8 nm), in the amorphous carbon layers allowed the Au atoms to come into contact with the CH_4 molecules, thus ensuring pyrolysis. The obvious change in the contrast in the amorphous carbon region indicates that the pyrolysis reaction occurred in the carbon portion, and it could have been catalyzed by a single-atom Au catalyst, thus demonstrating that single-atom Au and NPG co-catalyzed pyrolysis reactions. During pyrolysis, a new Au particle was formed, but it quickly disappeared (Fig. 6(b)), indicating that the nanoparticle and single-atom Au might not be independent of each other during the catalytic reactions. The co-catalysis process was proven via density functional theory (DFT) calculations and the mutual transformation of Au nanoparticles and single Au atoms (Fig. 6(c)). The reconstruction

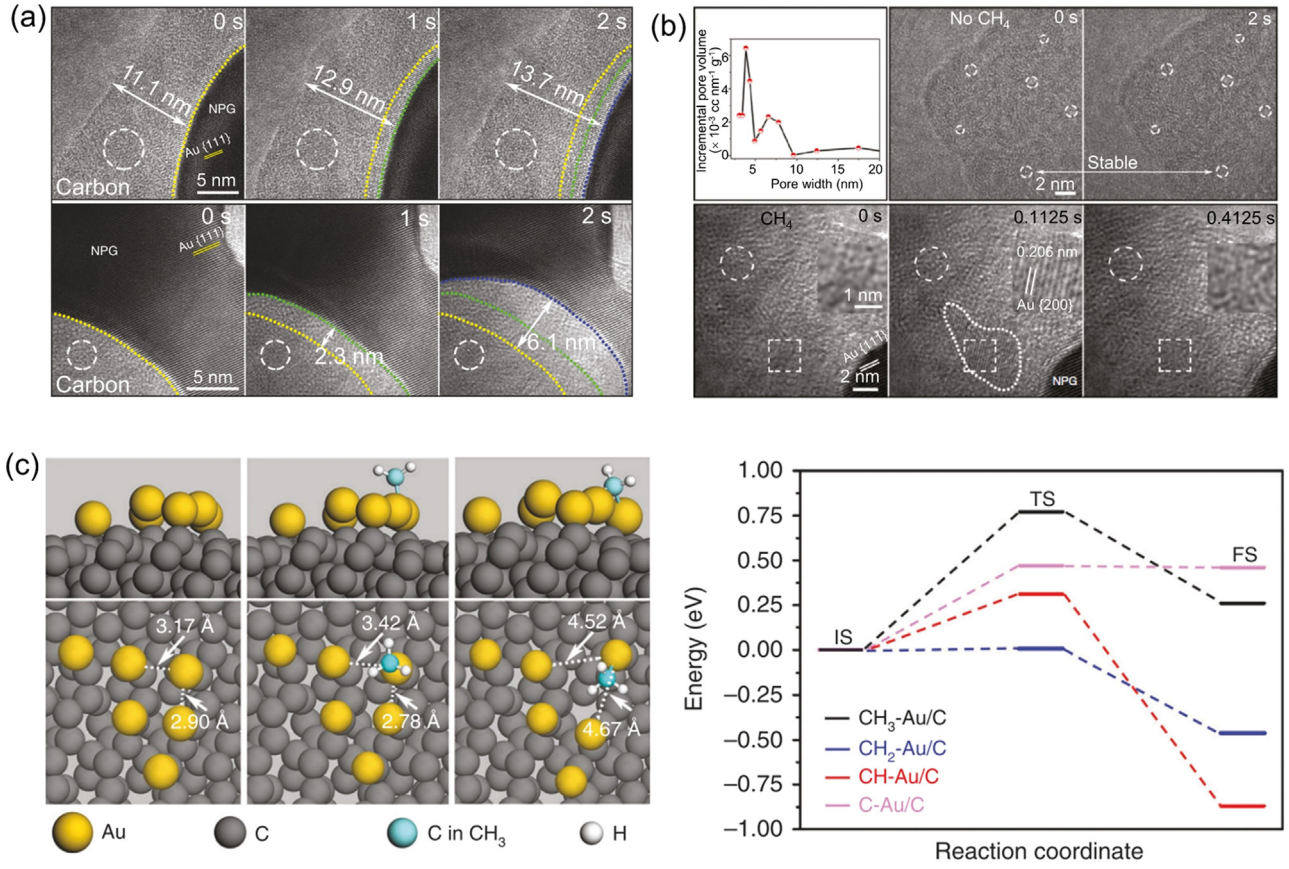

Fig. 6. (a)(b) In-situ dynamic observation of CH_4 pyrolysis over (a) nanoporous Au and (b) single-atom Au. Yellow, green, and blue dashed lines represent the positions of the surface at 0, 1, and 2 s, respectively. (c) Theoretical calculation of evolution of Au cluster on amorphous carbon.

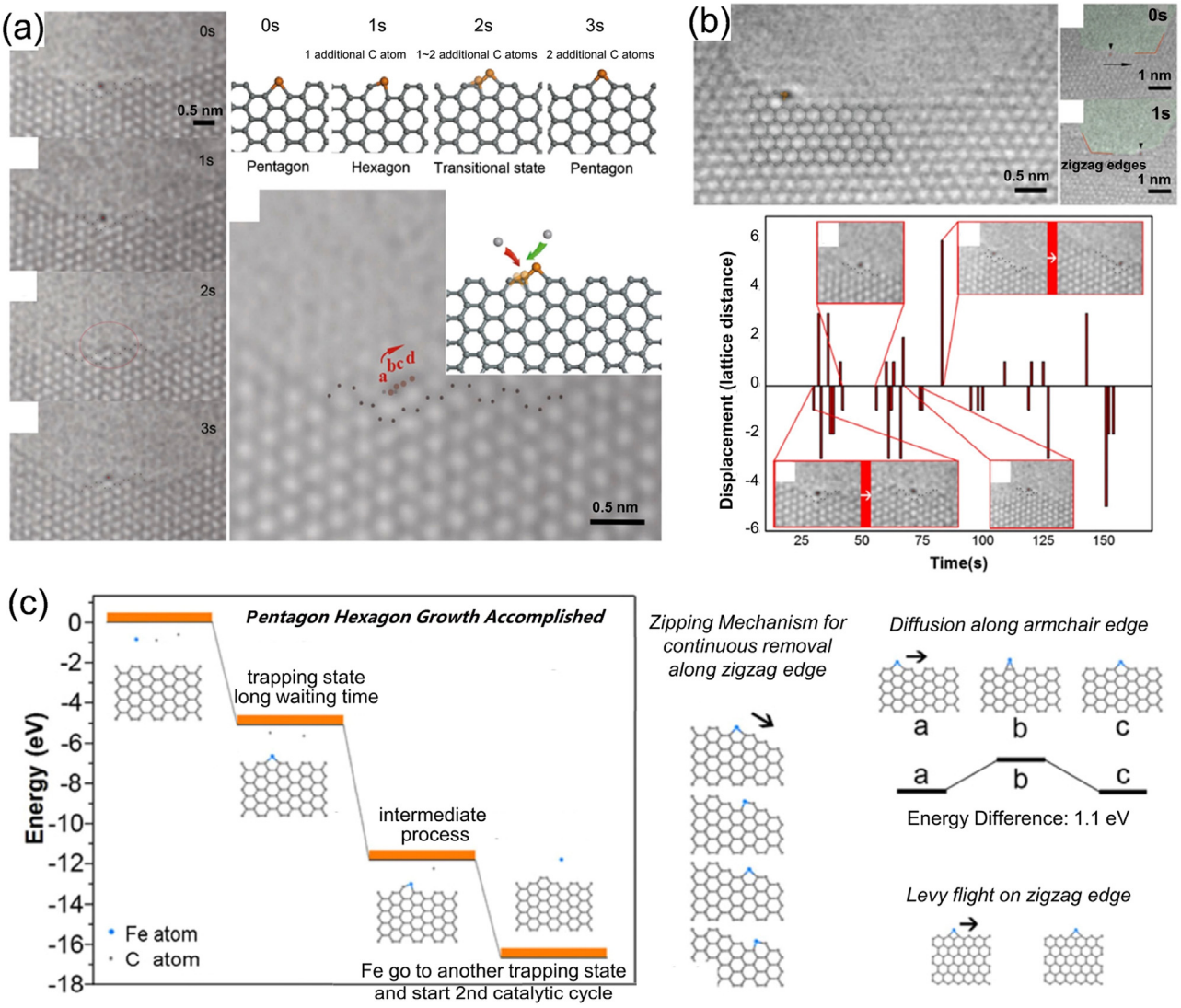

Fig. 7. (a) In-situ study of catalytic growth of graphene edge. (b) Single Fe atom located at zigzag edge and random displacement of Fe atom vs. time. (c) Theoretical catalytic and diffusion mechanism.

of a single-site Au catalyst into Au nanoclusters was also observed in Au/TiO_2, and it was induced by light illumination [100]. In addition, the synergistic catalytic performance between single atoms and neighboring clusters or single atoms has been investigated in various reactions [29,93,100,101].

3.2. Single-atom transition metals for catalyzing graphene growth

Transition metals such as Pt, Fe, Co, and Ni have a high carbon solubility at specific temperatures and are widely used for growing carbon nanotubes or carbon layers [102–105]. Rümmeli directly observed the diffusion behavior of a single Fe atom at graphene edges via in-situ TEM to reveal the growth mechanism of graphene over a single-atom Fe catalyst [42].

As shown in Fig. 7(a), the electron beam induces Fe atoms to diffuse to different locations along the graphene edge. Fe has a pentagonal structure. It absorbs some nearby carbon atoms to form a distorted hexagonal structure and moves toward the right. The movement of the single-atom Fe forms a dark shadow line (marked with a red circle); the movement finally stops at a nearby position, and the single-atom Fe forms a pentagon again. The corresponding atomic structural evolution process and the combination of the four frames are provided to facilitate a better understanding of the process. In addition, the Fe atoms exhibit different behaviors on the graphene zigzag and armchair edges, as revealed by experimental and theoretical calculations. For example, Fe atoms located at the zigzag edges can traverse large distances compared with the Fe atoms located at the zigzag edges. Additionally, the connection of carbon nanotubes and fullerenes to graphene was also observed with the in-situ TEM experiments; Cr atoms were used as the physical linkers [43]. The Cr atoms could drive the transformation of single-walled carbon nanotubes into fullerenes under electron irradiation. Scanning tunneling microscopy (STM) facilitated the direct observation of graphene growth on the nickel atoms [106].

3.3. Single-atom alloy for hydrogen dissociation and efficient C–H activation

Studies have concluded that Pt, Pd, Rh, and Ru possess hydrogenation-dissociation abilities and exhibit strong hydrogenation properties at mild temperatures [12,107–110]. Although Cu metals can activate H_2, the slow H_2 dissociation rate limits their application in various industrial reactions that do not require high pressures and temperatures. Alloying active components to an inert Cu substrate can be a favorable strategy for designing highly active catalysts.

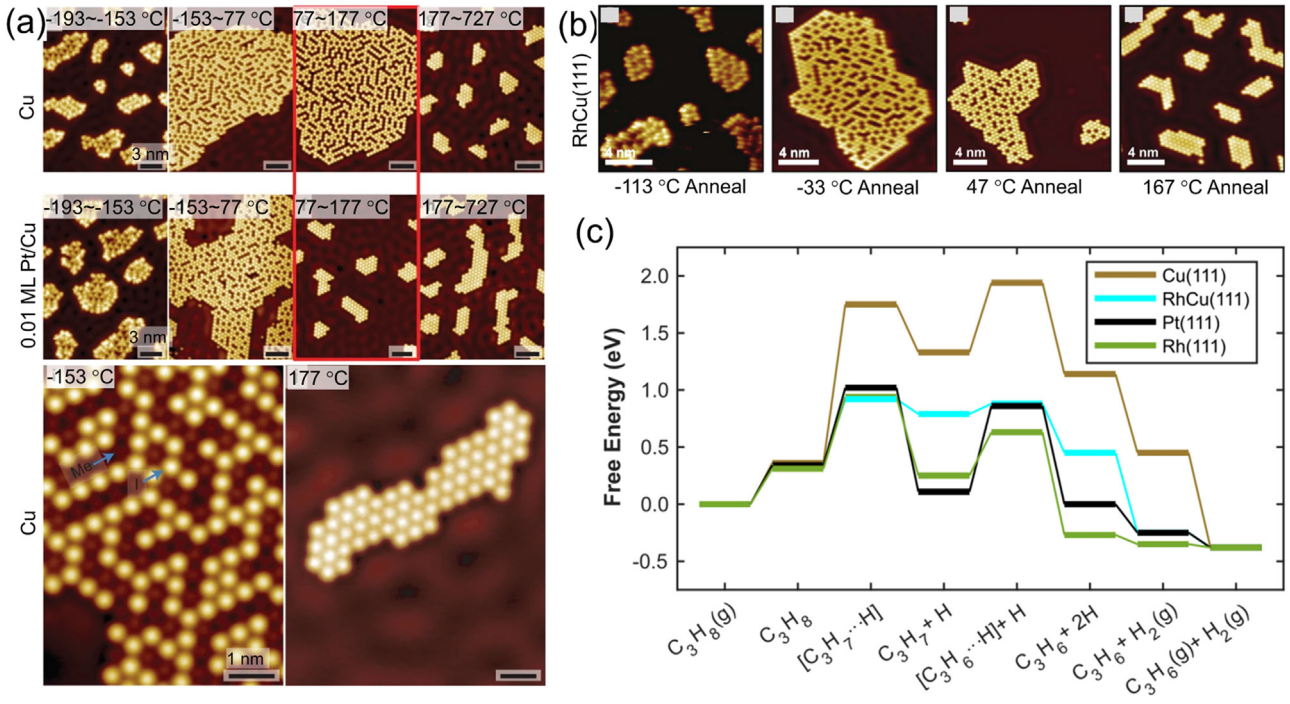

Fig. 8. (a)(b) STM imaging of lower-temperature C–H activation on different surfaces. In the STM images, the darker protrusion is methyl and brighter protrusion is iodine. (c) Free-energy profiles of single-atom Rh/Cu alloy and Cu (111) for the dehydrogenation of propane.

Sykes alloyed isolated Pd and Pt atoms onto a clean Cu surface using a physical vapor deposition strategy [12,107,111]. High-resolution STM analyses revealed the occurrence of hydrogen dissociation on the isolated noble metal atoms and spillover onto Cu substrates [12,111]. This facile hydrogen dissociation at individual active sites and the weak binding to the substrates resulted in an excellent catalytic performance in selective hydrogenation reactions [12,108,112–119]. In addition, Sykes discovered that single-atom alloys could efficiently catalyze C–H activation at low temperatures and display strong coke-resistant properties [28,120]. The authors conducted a temperature-programmed reaction (TPR) to study the C–H activation reaction by adding CH_3I to the single-atom alloy surface. The bright dots in the images represent I atoms, whereas the darker dots are CH_3 molecules. Intact disordered CH_3I clusters with intermixed bright and dark features were present in the images of both the Pt/Cu single-atom alloy and Cu surface at −193 °C, demonstrating that a temperature of −193 °C was insufficient to split the C–I bond (Fig. 8(a)). New well-defined ordered features with $\sqrt{3}\times\sqrt{3}R30^\circ$ structures were formed by increasing the temperature to −153 °C, and a few individual iodine atoms were separated; the separated iodine atoms were absorbed on Pt atoms from the two-dimensional clusters on the Pt/Cu surface. However, obvious changes were detected at higher temperatures (77–177 °C) for Cu (111) and single-atom Pt/Cu (111). Both bright and dark dots were present on Cu (111), and only bright dots remained in the $\sqrt{3}\times\sqrt{3}R30^\circ$ structure on the single-atom Pt/Cu (111). These experimental results demonstrated that the C–H activation of CH_3 on single-atom Pt/Cu(111) occurred at 77 °C, and it required a much higher temperature on Cu(111). A similar result was observed for the single-atom Rh/Cu alloy (Fig. 8(b)) [120]. DFT calculations indicated that single-atom Rh/Cu displayed much lower thermodynamic barriers for propane dehydrogenation process than pure Cu. Encouragingly, the activation barrier for propane on the single-atom Rh/Cu alloy was much lower than that on pure Pt and was similar to that on Rh (Fig. 8(c)). The weak binding of the intermediates to the single-atom alloy endowed this type of highly active catalyst with strong coking resistance.

3.4. Single-atom catalysts in energy fields

SACs have been extensively investigated in energy-related fields, such as hydrogen evolution [33], oxygen reduction [19,121], formic acid oxidation [122], CO_2 electroreduction [57], and Na–O_2 and Zn-air batteries [78]. However, most in-situ TEM studies focus on the single-atom transformation process at the preparation stage [57], and very few studies have investigated the catalytic behavior under reaction conditions [123,124]. Paul and Cherevko used a set of complementary analytical techniques to study the dissolution behavior of the as-synthesized Pt SACs, including online inductively coupled plasma mass spectrometry, identical location STEM, and XPS [124]. Two accelerated stress tests (ASTs) were designed and performed to investigate the stability of the Pt SACs. The extended load AST (eAST) demonstrated that most of the single Pt atoms remained at their original locations (Fig. 9(a)). After the combined “start–stop” and “load cycles” AST (cAST) from 0.6 to 1.5 V_{RHE}, some particles disappeared and other new particles or clusters formed, indicating the dissolution of particles and agglomeration of Pt SCAs into larger clusters (Fig. 9(a)). The oxidative potential of the ASTs could destabilize the S atoms on the supports, which, combined with the XPS results, could also lead to the dissolution of Pt. The isolated Pt atoms were prone to removal and agglomeration after the removal of the S ligands, demonstrating that S is the major stabilizing element for single Pt atoms; this phenomenon is similar to that which occurs in sulfur-doped carbon-supported Pt single atoms or particles [24,125,126]. Zhang et al. investigated the catalytic performance of single-atom Co/reduced graphene oxide (SA-Co/rGO) in solid-state Na–O_2 nanobatteries [123]. Spherical Na_2O_2 formed on the surface of SA-Co/rGO during discharging, and the rGO was completely covered by the products at the end of the discharging process. The spherical products easily decomposed into porous structures during the charging process. However, the formation and decomposition of spherical Na_2O_2 on the rGO were significantly slow. Three discharge-charge cycles were performed to investigate the cycling performance (Fig. 9(b)) [123].

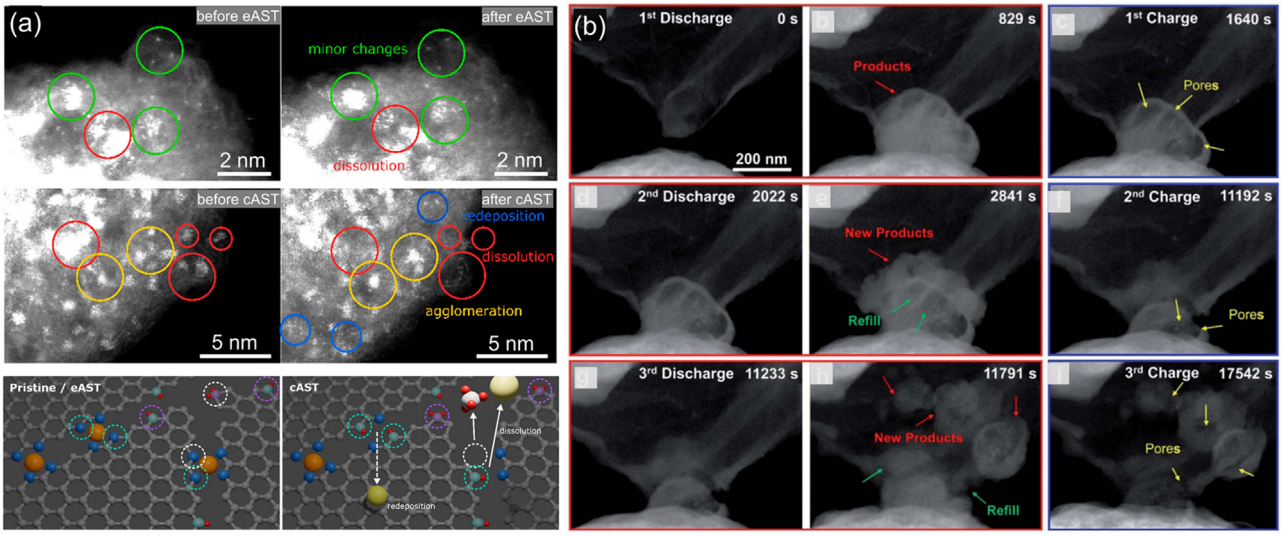

Fig. 9. (a) In-situ STEM observation of single-atom Pt in 1000 cycles of eAST and cAST. (b) SA-Co/rGO morphological evolution in Na–O_2 nanobattery during the first three discharge/charge cycles.

4. Summary and perspective

Over the last decade, numerous SACs have been synthesized using various strategies; they have been characterized by advanced techniques and displayed robust performance. Their efficacy was proven with theoretical calculations. The loading and thermal stability of the SACs do not appear to pose serious problems. Additionally, direct observations of the structural evolution of SACs have been reported. The evolution of metal particles into single atoms requires high temperatures to drive the release of metal atoms and strong binding sites to ensure the occurrence of the atomization and dispersion processes. Despite the excellent achievements in the direct observation of the behavior of SACs, there are many challenges that should be addressed. Here, we present the challenges and perspectives regarding these issues.

Most direct observations of the transformation of SACs have occurred at high temperatures; that is, these studies focused on SACs prepared at high temperatures. The formation mechanisms of SACs prepared at low or room temperatures remain unknown. Although some studies have been reported, the mechanism of the transformation of metal particles into single atoms remains unclear. For example, the transformation of Pt particles to single-atom Pt on reducible metal oxides requires a high temperature (> 800 °C) and an oxidizing atmosphere by emitting PtO_x species. This process can also occur in inert Ar through the competition between atomization and Oswald ripening over carbon-based carriers. Ru NPs supported on CeO_2 can also transform into single site Ru/CeO_2 at a very low temperature (210 °C). The release of metal atoms from the bulk material does not require high temperatures. The optimal temperature that provides the driving force for atomization remains unclear. The choice of annealing temperature used to fabricate single-atom catalysts is significantly influenced by the specific systems and atmospheres involved. Metal-support interactions play a significant role during the atomization and trapping processes; thus constructing optimum configuration motifs with strong chemical or thermal stability might be an effective strategy.

The in-situ observation of the dynamic behavior of SACs under environmental conditions still faces significant challenges. Most of the in-situ TEM or STEM studies focus on the transformation of SACs during preparation. However, further research is necessary to investigate the structural evolution of SACs during the reaction. Although numerous studies have reported the application of SACs in biomedicine, very few have reported their application in medicine under reaction conditions at the atomic scale. The therapeutic mechanism of SACs in medicine still needs to be elucidated. Single atoms are not easily observed under a bright field, whereas the frames or structures of the reactants and intermediates cannot be recognized under a dark field. Thus, new techniques or strategies should be developed to in-situ observe the dynamic changes of SACs, which will undoubtedly assist in revealing the reaction mechanism. Dimers and trimers with multiple single metals have also been recently developed, and the coexistence of multiple metals results in excellent catalytic performance. In-situ observations of the dimer transformation process have seldom been reported. Although the structure of single atoms could be clearly observed using TEM, the elucidation of the catalytic behavior and mechanism was still difficult because of the complications of electron and/or mass transfer. The ligands or electronic properties cannot be ignored and require a combination of other in-situ techniques, such as FTIR, XAS, and XPS. A large number of studies should be performed in the future to clarify the transformation and reaction mechanism via in-situ TEM.

Declaration of Competing Interest

The authors declare that they have no known competing financial interests or personal relationships that could have appeared to influence the work reported in this paper.

Acknowledgements

We would like to acknowledge funding support from the National Natural Science Foundation of China (52204255), Jiangsu Key Laboratory of Coal-based Greenhouse Gas Control and Utilization (PCSX202201), China Postdoctoral Science Foundation (2020M682764), and the Yangzhou University Start-up Foundation.

References

[1] Z. Li, S. Ji, Y. Liu, X. Cao, S. Tian, Y. Chen, Z. Niu, Y. Li, Well-defined materials materials for heterogeneous catalysis: From nanoparticles to isolated single-atom sites, Chem. Rev. 120 (2020) 623–682.
[2] L. Liu, A. Corma, Metal catalysts for heterogeneous catalysis: From single atoms to nanoclusters and nanoparticles, Chem. Rev. 118 (2018) 4981–5079.
[3] X.F. Yang, A. Wang, B. Qiao, J. Li, J. Liu, T. Zhang, Single-atom catalysts: A new frontier in heterogeneous catalysis, Acc. Chem. Res. 46 (2013) 1740–1748.
[4] B. Qiao, A. Wang, X. Yang, L.F. Allard, Z. Jiang, Y. Cui, J. Liu, J. Li, T. Zhang, Single-atom catalysis of CO oxidation using Pt_1/FeO_x, Nat. Chem. 3 (2011) 634–641.

[5] J. Jones, H. Xiong, A.T. DeLaRiva, E.J. Peterson, P. Hien, S.R. Challa, G. Qi, S. Oh, M.H. Wiebenga, X.I.P. Hernandez, Y. Wang, A.K. Datye, Thermally stable single-atom platinum-on-ceria catalysts via atom trapping, Science 353 (2016) 150–154.
[6] P. Liu, Y. Zhao, R. Qin, S. Mo, G. Chen, L. Gu, D.M. Chevrier, P. Zhang, Q. Guo, D. Zang, B. Wu, G. Fu, N. Zheng, Photochemical route for synthesizing atomically dispersed palladium catalysts, Science 352 (2016) 797–801.
[7] G. Malta, S.A. Kondrat, S.J. Freakley, C.J. Davies, L. Lu, S. Dawson, A. Thetford, E.K. Gibson, D.J. Morgan, W. Jones, P.P. Wells, P. Johnston, C.R.A. Catlow, C.J. Kiely, G.J. Hutchings, Identification of single-site gold catalysis in acetylene hydrochlorination, Science 355 (2017) 1399–1402.
[8] L. Nie, D. Mei, H. Xiong, B. Peng, Z. Ken, X.I.P. Hernandez, A. DeLariva, M. Wang, M.H. Engelhard, L. Kovarik, A.K. Datye, Y. Wang, Activation of surface lattice oxygen in single-atom Pt/CeO_2 for low-temperature CO oxidation, Science 358 (2017) 1419–1423.
[9] L. Wang, J. Wang, X. Gao, C. Chen, Y. Da, S. Wang, J. Yang, Z. Wang, J. Song, T. Yao, W. Zhou, H. Zhou, Y. Wu, Periodic one-dimensional single-atom arrays, J. Am. Chem. Soc. 144 (2022) 15999–16005.
[10] X. Cui, W. Li, P. Ryabchuk, K. Junge, M. Beller, Bridging homogeneous and heterogeneous catalysis by heterogeneous single-metal-site catalysts, Nat. Catal. 1 (2018) 385–397.
[11] F. Huang, Y. Deng, Y. Chen, X. Cai, M. Peng, Z. Jia, J. Xie, D. Xiao, X. Wen, N. Wang, Z. Jiang, H. Liu, D. Ma, Anchoring Cu_1 species over nanodiamond-graphene for semi-hydrogenation of acetylene, Nat. Commun. 10 (2019) 4431.
[12] G. Kyriakou, M.B. Boucher, A.D. Jewell, E.A. Lewis, T.J. Lawton, A.E. Baber, H.L. Tierney, M. Flytzani-Stephanopoulos, E.C.H. Sykes, Isolated metal atom geometries as a strategy for selective heterogeneous hydrogenations, Science 335 (2012) 1209–1212.
[13] G. Sun, Z.-J. Zhao, R. Mu, S. Zha, L. Li, S. Chen, K. Zang, J. Luo, Z. Li, S.C. Purdy, A.J. Kropf, J.T. Miller, L. Zeng, J. Gong, Breaking the scaling relationship via thermally stable Pt/Cu single atom alloys for catalytic dehydrogenation, Nat. Commun. 9 (2018) 4454.
[14] L.N. Cao, W. Liu, Q.Q. Luo, R.T. Yin, B. Wang, J. Weissenrieder, M. Soldemo, H. Yan, Y. Lin, Z.H. Sun, C. Ma, W.H. Zhang, S. Chen, H.W. Wang, Q.Q. Guan, T. Yao, S.Q. Wei, J.L. Yang, J.L. Lu, Atomically dispersed iron hydroxide anchored on Pt for preferential oxidation of CO in H_2, Nature 565 (2019) 631–635.
[15] K. Ding, A. Gulec, A.M. Johnson, N.M. Schweitzer, G.D. Stucky, L.D. Marks, P.C. Stair, Identification of active sites in CO oxidation and water-gas shift over supported Pt catalysts, Science 350 (2015) 189–192.
[16] M. Yang, S. Li, Y. Wang, J.A. Herron, Y. Xu, L.F. Allard, S. Lee, J. Huang, M. Mavrikakis, M. Flytzani-Stephanopoulos, Catalytically active Au-$O(OH)_x$-species stabilized by alkali ions on zeolites and mesoporous oxides, Science 346 (2014) 1498–1501.
[17] X.F. Li, Q.K. Li, J. Cheng, L. Liu, Q. Yan, Y. Wu, X.H. Zhang, Z.Y. Wang, Q. Qiu, Y. Luo, Conversion of dinitrogen to ammonia by FeN_3-embedded graphene, J. Am. Chem. Soc. 138 (2016) 8706–8709.
[18] A. Zitolo, V. Goellner, V. Armel, M.T. Sougrati, T. Mineva, L. Stievano, E. Fonda, F. Jaouen, Identification of catalytic sites for oxygen reduction in iron- and nitrogen-doped graphene materials, Nat. Mater. 14 (2015) 937.
[19] C.H. Choi, M. Kim, H.C. Kwon, S.J. Cho, S. Yun, H.T. Kim, K.J.J. Mayrhofer, H. Kim, M. Choi, Tuning selectivity of electrochemical reactions by atomically dispersed platinum catalyst, Nat. Commun. 7 (2016) 10922.
[20] P.N. Duchesne, Z.Y. Li, C.P. Deming, V. Fung, X. Zhao, J. Yuan, T. Regier, A. Aldalbahi, Z. Almarhoon, S. Chen, D. Jiang, N. Zheng, P. Zhang, Golden single-atomic-site platinum electrocatalysts, Nat. Mater. 17 (2018) 1033.
[21] N. Zhang, X. Zhang, L. Tao, P. Jiang, C. Ye, R. Lin, Z. Huang, A. Li, D. Pang, H. Yan, Y. Wang, P. Xu, S. An, Q. Zhang, L. Liu, S. Du, X. Han, D. Wang, Y. Li, Silver single-atom catalyst for efficient electrochemical CO_2 reduction synthesized from thermal transformation and surface reconstruction, Angew. Chem. Int. Ed. 60 (2021) 6170–6176.
[22] D. Liu, X. Li, S. Chen, H. Yan, C. Wang, C. Wu, Y.A. Haleem, S. Duan, J. Lu, B. Ge, P.M. Ajayan, Y. Luo, J. Jiang, L. Song, Atomically dispersed platinum supported on curved carbon supports for efficient electrocatalytic hydrogen evolution, Nature Energy 4 (2019) 512–518.
[23] M. Huo, L. Wang, Y. Wang, Y. Chen, J. Shi, Nanocatalytic tumor therapy by single-atom catalysts, ACS Nano 13 (2019) 2643–2653.
[24] L. Wang, M.X. Chen, Q.Q. Yan, S.L. Xu, S.Q. Chu, P. Chen, Y. Lin, H.W. Liang, A sulfur-tethering synthesis strategy toward high-loading atomically dispersed noble metal catalysts, Sci. Adv. 5 (2019) eaax6322.
[25] L. Lin, Q. Yu, M. Peng, A. Li, S. Yao, S. Tian, X. Liu, A. Li, Z. Jiang, R. Gao, X. Han, Y.W. Li, X.D. Wen, W. Zhou, D. Ma, Atomically dispersed Ni/alpha-MoC catalyst for hydrogen production from methanol/water, J. Am. Chem. Soc. 143 (2021) 309–317.
[26] Q. Sun, N. Wang, T. Zhang, R. Bai, A. Mayoral, P. Zhang, Q. Zhang, O. Terasaki, J. Yu, Zeolite-encaged single-stom rhodium satalysts: Highly-efficient hydrogen generation and shape-selective tandem hydrogenation of nitroarenes, Angew. Chem. Int. Ed. 58 (2019) 18570–18576.
[27] M.D. Marcinkowski, J. Liu, C.J. Murphy, M.L. Liriano, N.A. Wasio, F.R. Lucci, M. Flytzani-Stephanopoulos, E.C.H. Sykes, Selective formic acid dehydrogenation on Pt-Cu single-atom alloys, ACS Catal. 7 (2017) 413–420.
[28] M.D. Marcinkowski, M.T. Darby, J. Liu, J.M. Wimble, F.R. Lucci, S. Lee, A. Michaelides, M. Flytzani-Stephanopoulos, M. Stamatakis, E.C.H. Sykes, Pt/Cu single-atom alloys as coke-resistant catalysts for efficient C-H activation, Nat Chem 10 (2018) 325–332.
[29] H. Li, L. Wang, Y. Dai, Z. Pu, Z. Lao, Y. Chen, M. Wang, X. Zheng, J. Zhu, W. Zhang, R. Si, C. Ma, J. Zeng, Synergetic interaction between neighbouring platinum monomers in CO_2 hydrogenation, Nat. Nanotechnol. 13 (2018) 411–417.
[30] H.S. Wei, X.Y. Liu, A.Q. Wang, L.L. Zhang, B.T. Qiao, X.F. Yang, Y.Q. Huang, S. Miao, J.Y. Liu, T. Zhang, FeO_x-supported platinum single-atom and pseudo-single-atom catalysts for chemoselective hydrogenation of functionalized nitroarenes, Nat. Commun. 5 (2014) 5634.
[31] H. Yan, H. Cheng, H. Yi, Y. Lin, T. Yao, C. Wang, J. Li, S. Wei, J. Lu, Single-atom Pd_1/graphene catalyst achieved by atomic layer deposition: Remarkable performance in selective hydrogenation of 1,3-butadiene, J. Am. Chem. Soc. 137 (2015) 10484–10487.
[32] Z. Li, Y. Chen, S. Ji, Y. Tang, W. Chen, A. Li, J. Zhao, Y. Xiong, Y. Wu, Y. Gong, T. Yao, W. Liu, L. Zheng, J. Dong, Y. Wang, Z. Zhuang, W. Xing, C.T. He, C. Peng, W.C. Cheong, Q. Li, M. Zhang, Z. Chen, N. Fu, X. Gao, W. Zhu, J. Wan, J. Zhang, L. Gu, S. Wei, P. Hu, J. Luo, J. Li, C. Chen, Q. Peng, X. Duan, Y. Huang, X.M. Chen, D. Wang, Y. Li, Iridium single-atom catalyst on nitrogen-doped carbon for formic acid oxidation synthesized using a general host–guest strategy, Nat. Chem. 12 (2020) 764–772.
[33] H.W. Liang, S. Bruller, R. Dong, J. Zhang, X. Feng, K. Mullen, Molecular metal-N_x centres in porous carbon for electrocatalytic hydrogen evolution, Nat. Commun. 6 (2015) 7992.
[34] X. He, Q. He, Y. Deng, M. Peng, H. Chen, Y. Zhang, S. Yao, M. Zhang, D. Xiao, D. Ma, B. Ge, H. Ji, A versatile route to fabricate single atom catalysts with high chemoselectivity and regioselectivity in hydrogenation, Nat. Commun. 10 (2019) 3663.
[35] H. Wei, K. Huang, D. Wang, R. Zhang, B. Ge, J. Ma, B. Wen, S. Zhang, Q. Li, M. Lei, C. Zhang, J. Irawan, L.M. Liu, H. Wu, Iced photochemical reduction to synthesize atomically dispersed metals by suppressing nanocrystal growth, Nat. Commun. 8 (2017) 1490.
[36] Y. Qu, B. Chen, Z. Li, X. Duan, L. Wang, Y. Lin, T. Yuan, F. Zhou, Y. Hu, Z. Yang, C. Zhao, J. Wang, C. Zhao, Y. Hu, G. Wu, Q. Zhang, Q. Xu, B. Liu, P. Gao, R. You, W. Huang, L. Zheng, L. Gu, Y. Wu, Y. Li, Thermal emitting strategy to synthesize atomically dispersed Pt metal sites from bulk Pt metal, J. Am. Chem. Soc. 141 (2019) 4505–4509.
[37] Z. Yang, B. Chen, W. Chen, Y. Qu, F. Zhou, C. Zhao, Q. Xu, Q. Zhang, X. Duan, Y. Wu, Directly transforming copper (I) oxide bulk into isolated single-atom copper sites catalyst through gas-transport approach, Nat. Commun. 10 (2019) 3734.
[38] L. Zhang, R. Si, H. Liu, N. Chen, Q. Wang, K. Adair, Z. Wang, J. Chen, Z. Song, J. Li, M.N. Banis, R. Li, T.K. Sham, M. Gu, L.M. Liu, G.A. Botton, X. Sun, Atomic layer deposited Pt-Ru dual-metal dimers and identifying their active sites for hydrogen evolution reaction, Nat. Commun. 10 (2019) 4936.
[39] S. Tian, Q. Fu, W. Chen, Q. Feng, Z. Chen, J. Zhang, W.C. Cheong, R. Yu, L. Gu, J. Dong, J. Luo, C. Chen, Q. Peng, C. Draxl, D. Wang, Y. Li, Carbon nitride supported Fe-2 cluster catalysts with superior performance for alkene epoxidation, Nat. Commun. 9 (2018) 2353.
[40] F. Huang, M. Peng, Y. Chen, X. Cai, X. Qin, N. Wang, D. Xiao, L. Jin, G. Wang, X.-D. Wen, H. Liu, D. Ma, Low-temperature acetylene semi-hydrogenation over the Pd_1–Cu_1 dual-atom catalyst, J. Am. Chem. Soc. 144 (2022) 18485–18493.
[41] L. Wang, P. Yin, W.J. Zeng, S.L. Xu, P. Chen, H.W. Liang, Bulky nanodiamond–confined synthesis of sub-5 nanometer ordered intermetallic Pd_3Pb catalysts, Nano Res. 15 (2022) 4973–4979.
[42] J. Zhao, Q. Deng, S.M. Avdoshenko, L. Fu, J. Eckert, M.H. Rümmeli, Direct in situ observations of single Fe atom catalytic processes and anomalous diffusion at graphene edges, Proc. Natl. Acad. Sci. USA 111 (2014) 15641.
[43] L. Zhao, H.Q. Ta, A. Dianat, A. Soni, A. Fediai, W. Yin, T. Gemming, B. Trzebicka, G. Cuniberti, Z. Liu, A. Bachmatiuk, M.H. Rummeli, In situ electron driven carbon nanopillar-fullerene transformation through Cr atom mediation, Nano Lett. 17 (2017) 4725–4732.
[44] L. Lin, Q. Yu, M. Peng, A. Li, S. Yao, S. Tian, X. Liu, A. Li, Z. Jiang, R. Gao, X. Han, Y.W. Li, X.D. Wen, W. Zhou, D. Ma, Atomically dispersed Ni/α-MoC catalyst for hydrogen production from methanol/water, J. Am. Chem. Soc. 143 (2021) 309–317.
[45] W. Lei, Z. Lei, Z. Luyao, Y. Yulong, W. Kun, Y. Boyuan, Z. Xin, Y. Feng, Direct environmental TEM observation of silicon diffusion-induced strong metal-silica interaction for boosting CO_2 hydrogenation, Nano Res 16 (2023) 2209–2217.
[46] L. Wang, W. Zhang, S. Wang, Z. Gao, Z. Luo, X. Wang, R. Zeng, A. Li, H. Li, M. Wang, X. Zheng, J. Zhu, W. Zhang, C. Ma, R. Si, J. Zeng, Atomic-level insights in optimizing reaction paths for hydroformylation reaction over Rh/CoO single-atom catalyst, Nat. Commun. 7 (2016) 14036.
[47] X. Li, W. Bi, M. Chen, Y. Sun, H. Ju, W. Yan, J. Zhu, X. Wu, W. Chu, C. Wu, Y. Xie, Exclusive Ni-N_4 sites realize near-unity CO selectivity for electrochemical CO_2 reduction, J. Am. Chem. Soc. 139 (2017) 14889–14892.
[48] H. Fei, J. Dong, Y. Feng, C.S. Allen, C. Wan, B. Volosskiy, M. Li, Z. Zhao, Y. Wang, H. Sun, P. An, W. Chen, Z. Guo, C. Lee, D. Chen, I. Shakir, M. Liu, T. Hu, Y. Li, A.I. Kirkland, X. Duan, Y. Huang, General synthesis and definitive structural identification of MN_4C_4 single-atom catalysts with tunable electrocatalytic activities, Nat. Catal. 1 (2018) 63–72.
[49] R. Lang, T. Li, D. Matsumura, S. Miao, Y. Ren, Y.T. Cui, Y. Tan, B. Qiao, L. Li, A. Wang, X. Wang, T. Zhang, Hydroformylation of olefins by a rhodium single-atom catalyst with activity comparable to $RhCl(PPh_3)_3$, Angew. Chem. Int. Ed. 55 (2016) 16054–16058.
[50] W. Yuan, Y. Wang, H. Li, H. Wu, Z. Zhang, A. Selloni, C. Sun, Real-time observation of reconstruction dynamics on TiO_2(001) surface under oxygen via an environmental transmission electron microscope, Nano Lett. 16 (2016) 132–137.
[51] W. Yuan, B. Zhu, X.-Y. Li, T.W. Hansen, Y. Ou, K. Fang, H. Yang, Z. Zhang, J.B. Wagner, Y. Gao, Y. Wang, Visualizing H_2O molecules reacting at TiO_2 active sites with transmission electron microscopy, Science 367 (2020) 428.

[52] Y. Niu, B. Zhang, In situ investigation of nanocatalysts in gas atmosphere by transmission electron microscopy, Curr. Opin. Green. Sustain. Chem. 22 (2020) 22–28.
[53] F. Tao, P.A. Crozier, Atomic-scale observations of catalyst structures under reaction conditions and during catalysis, Chem. Rev. 116 (2016) 3487–3539.
[54] H. Zhao, Y. Zhu, H. Ye, Y. He, H. Li, Y. Sun, F. Yang, R. Wang, Atomic-scale structure dynamics of nanocrystals revealed by in-situ and environmental transmission electron microscopy, Adv. Mater. (2022) 2206911.
[55] L. Wang, X. Zhao, X. Yang, K. Wang, F. Yang, Thermally stable single atom catalysts: From concept to in situ study, Funct. Mater. Lett. 14 (2021) 2130007.
[56] S. Wei, A. Li, J.C. Liu, Z. Li, W. Chen, Y. Gong, Q. Zhang, W.C. Cheong, Y. Wang, L. Zheng, H. Xiao, C. Chen, D. Wang, Q. Peng, L. Gu, X. Han, J. Li, Y. Li, Direct observation of noble metal nanoparticles transforming to thermally stable single atoms, Nat. Nanotechnol. 13 (2018) 856–861.
[57] J. Yang, Z. Qiu, C. Zhao, W. Wei, W. Chen, Z. Li, Y. Qu, J. Dong, J. Luo, Z. Li, Y. Wu, In situ thermal atomization to convert supported nickel nanoparticles into surface-bound nickel single-atom catalysts, Angew. Chem. Int. Ed. 57 (2018) 14095–14100.
[58] L. Zhang, Y. Li, L. Zhang, K. Wang, Y. Li, L. Wang, X. Zhang, F. Yang, Z. Zheng, Direct visualization of the evolution of a single-atomic cobalt catalyst from melting nanoparticles with carbon dissolution, Adv, Sci 9 (2022) e2200592.
[59] J. Liu, F.R. Lucci, M. Yang, S. Lee, M.D. Marcinkowski, A.J. Therrien, C.T. Williams, E.C.H. Sykes, M. Flytzani-Stephanopoulos, Tackling CO poisoning with single-atom alloy catalysts, J. Am. Chem. Soc. 138 (2016) 6396–6399.
[60] R. Lang, W. Xi, J.C. Liu, Y.T. Cui, T. Li, A.F. Lee, F. Chen, Y. Chen, L. Li, L. Li, J. Lin, S. Miao, X. Liu, A.Q. Wang, X. Wang, J. Luo, B. Qiao, J. Li, T. Zhang, Non defect-stabilized thermally stable single-atom catalyst, Nat. Commun. 10 (2019) 234.
[61] P.Q. Yin, T. Yao, Y. Wu, L.R. Zheng, Y. Lin, W. Liu, H.X. Ju, J.F. Zhu, X. Hong, Z.X. Deng, G. Zhou, S.Q. Wei, Y.D. Li, Single cobalt atoms with precise N-coordination as superior oxygen reduction reaction catalysts, Angew. Chem. Int. Ed. 55 (2016) 10800–10805.
[62] J. Gu, C.S. Hsu, L. Bai, H.M. Chen, X. Hu, Atomically dispersed Fe^{3+} sites catalyze efficient CO_2 electroreduction to CO, Science 364 (2019) 1091.
[63] D. Zhao, Z. Chen, W. Yang, S. Liu, X. Zhang, Y. Yu, W.C. Cheong, L. Zheng, F. Ren, G. Ying, X. Cao, D. Wang, Q. Peng, G. Wang, C. Chen, MXene (Ti_3C_2) vacancy-confined single-atom catalyst for efficient functionalization of CO_2, J. Am. Chem. Soc. 141 (2019) 4086–4093.
[64] Z. Chen, E. Vorobyeva, S. Mitchell, E. Fako, M.A. Ortuno, N. Lopez, S.M. Collins, P.A. Midgley, S. Richard, G. Vile, J. Perez-Ramirez, A heterogeneous single-atom palladium catalyst surpassing homogeneous systems for Suzuki coupling, Nat. Nanotechnol. 13 (2018) 702–707.
[65] Q. Sun, N. Wang, T. Zhang, R. Bai, A. Mayoral, P. Zhang, Q. Zhang, O. Terasaki, J. Yu, Zeolite-encaged single-atom rhodium catalysts: Highly-efficient hydrogen generation and shape-selective tandem hydrogenation of nitroarenes, Angew. Chem. Int. Ed. 58 (2019) 18570–18576.
[66] A. Cao, G. Veser, Exceptional high-temperature stability through distillation-like self-stabilization in bimetallic nanoparticles, Nat. Mater. 9 (2010) 75–81.
[67] L. Wang, P. Yin, L.L. Zhang, S.C. Shen, S.L. Xu, P. Chen, H.W. Liang, Nitrogen-fixing of ultrasmall Pd-based bimetallic nanoclusters on carbon supports, J. Catal. 389 (2020) 297–304.
[68] L. Wang, S. Lyu, P. Zhang, X. Tian, D. Wang, W. Huang, Z. Liu, Nitrogen-bonded ultrasmall palladium clusters over the nitrogen-doped carbon for promoting Suzuki cross-coupling reactions, Adv. Compos. Hybrid Mater. 5 (2022) 1396–1403.
[69] Y. Physical Review B. Dai, P. Lu, Z. Cao, C.T. Campbell, Y. Xia, The physical chemistry and materials science behind sinter-resistant catalysts, Chem. Soc. Rev. 47 (2018) 4314–4331.
[70] E.D. Goodman, J.A. Schwalbe, M. Cargnello, Mechanistic understanding and the rational design of sinter-resistant heterogeneous catalysts, ACS Catal 7 (2017) 7156–7173.
[71] C. Carrillo, T.R. Johns, H. Xiong, A. DeLaRiva, S.R. Challa, R.S. Goeke, K. Artyushkova, W. Li, C.H. Kim, A.K. Datye, Trapping of mobile Pt species by PdO nanoparticles under oxidizing conditions, J. Phys. Chem. Lett. 5 (2014) 2089–2093.
[72] R. Lang, W. Xi, J.C. Liu, Y.T. Cui, T. Li, A.F. Lee, F. Chen, Y. Chen, L. Li, L. Li, J. Lin, S. Miao, X. Liu, A.Q. Wang, X. Wang, J. Luo, B. Qiao, J. Li, T. Zhang, Non defect-stabilized thermally stable single-atom catalyst, Nat. Commun. 10 (2019).
[73] K. Liu, X. Zhao, G. Ren, T. Yang, Y. Ren, A.F. Lee, Y. Su, X. Pan, J. Zhang, Z. Chen, J. Yang, X. Liu, T. Zhou, W. Xi, J. Luo, C. Zeng, H. Matsumoto, W. Liu, Q. Jiang, K. Wilson, A. Wang, B. Qiao, W. Li, T. Zhang, Strong metal-support interaction promoted scalable production of thermally stable single-atom catalysts, Nat. Commun. 11 (2020) 1263.
[74] Y. Zhao, H. Zhou, X. Zhu, Y. Qu, C. Xiong, Z. Xue, Q. Zhang, X. Liu, F. Zhou, X. Mou, W. Wang, M. Chen, Y. Xiong, X. Lin, Y. Lin, W. Chen, H.J. Wang, Z. Jiang, L. Zheng, T. Yao, J. Dong, S. Wei, W. Huang, L. Gu, J. Luo, Y. Li, Y. Wu, Simultaneous oxidative and reductive reactions in one system by atomic design, Nat. Catal. 4 (2021) 134–143.
[75] G. Yang, J. Zhu, P. Yuan, Y. Hu, G. Qu, B.A. Lu, X. Xue, H. Yin, W. Cheng, J. Cheng, W. Xu, J. Li, J. Hu, S. Mu, J.N. Zhang, Regulating Fe-spin state by atomically dispersed Mn-N in Fe-N-C catalysts with high oxygen reduction activity, Nat. Commun. 12 (2021) 1734.
[76] N. Zhang, T. Zhou, M. Chen, H. Feng, R. Yuan, C.A. Zhong, W. Yan, Y. Tian, X. Wu, W. Chu, C. Wu, Y. Xie, High-purity pyrrole-type FeN_4 sites as a superior oxygen reduction electrocatalyst, Energy Environ. Sci. 13 (2020) 111–118.
[77] K. Yuan, D. Lutzenkirchen-Hecht, L. Li, L. Shuai, Y. Li, R. Cao, M. Qiu, X. Zhuang, M.K.H. Leung, Y. Chen, U. Scherf, Boosting oxygen reduction of single iron active sites via geometric and electronic engineering: Nitrogen and phosphorus dual coordination, J. Am. Chem. Soc. 142 (2020) 2404–2412.
[78] Z. Zhang, X. Zhao, S. Xi, L. Zhang, Z. Chen, Z. Zeng, M. Huang, H. Yang, B. Liu, S.J. Pennycook, P. Chen, Atomically dispersed cobalt trifunctional electrocatalysts with tailored coordination environment for flexible rechargeable Zn–air battery and self-driven water splitting, Adv. Energy Mater. 10 (2020) 2002896.
[79] L.W. Chen, Z.Y. Wu, H. Nan, L. Wang, S.Q. Chu, H.W. Liang, A metal-catalyzed thermal polymerization strategy toward atomically dispersed catalysts, Chem. Commun. 55 (2019) 11579–11582.
[80] P. Yin, T. Yao, Y. Wu, L. Zheng, Y. Lin, W. Liu, H. Ju, J. Zhu, X. Hong, Z. Deng, G. Zhou, S. Wei, Y. Li, Single cobalt atoms with precise N-coordination as superior oxygen reduction reaction catalysts, Angew. Chem. Int. Ed. 55 (2016) 10800–10805.
[81] C. Zhao, X. Dai, T. Yao, W. Chen, X. Wang, J. Wang, J. Yang, S. Wei, Y. Wu, Y. Li, Ionic exchange of metal organic frameworks to access single nickel sites for efficient electroreduction of CO_2, J. Am. Chem. Soc. 139 (2017) 8078–8081.
[82] Z. Geng, Y. Liu, X. Kong, P. Li, K. Li, Z. Liu, J. Du, M. Shu, R. Si, J. Zeng, Achieving a record-high yield rate of 120.9 mu g_{NH3} $mg_{cat.}^{-1}$ h^{-1} for N_2 electrochemical reduction over Ru single-atom catalysts, Adv. Mater. 30 (2018) e1803498.
[83] X. Mi, P. Wang, S. Xu, L. Su, H. Zhong, H. Wang, Y. Li, S. Zhan, Almost 100% peroxymonosulfate conversion to singlet oxygen on single-atom CoN_{2+2} sites, Angew. Chem. Int. Ed. 60 (2020) 4588–4593.
[84] Y.N. Gong, L. Jiao, Y. Qian, C.Y. Pan, L. Zheng, X. Cai, B. Liu, S.H. Yu, H.L. Jiang, Regulating the coordination environment of MOF-templated single-atom nickel electrocatalysts for boosting CO_2 reduction, Angew. Chem. Int. Ed. 59 (2020) 2705–2709.
[85] Y. Chen, R. Gao, S. Ji, H. Li, K. Tang, P. Jiang, H. Hu, Z. Zhang, H. Hao, Q. Qu, X. Liang, W. Chen, J. Dong, D. Wang, Y. Li, Atomic-level modulation of electronic density of metal-organic frameworks-derived Co single-atom sites to enhance oxygen reduction performance, Angew. Chem. Int. Ed. 60 (2020) 3212–3221.
[86] H. Zhou, Y. Zhao, J. Xu, H. Sun, Z. Li, W. Liu, T. Yuan, W. Liu, X. Wang, W.-C. Cheong, Z. Wang, X. Wang, C. Zhao, Y. Yao, W. Wang, F. Zhou, M. Chen, B. Jin, R. Sun, J. Liu, X. Hong, T. Yao, S. Wei, J. Luo, Y. Wu, Recover the activity of sintered supported catalysts by nitrogen-doped carbon atomization, Nat. Commun. 11 (2020) 335.
[87] H. Zhou, Y. Zhao, J. Gan, J. Xu, Y. Wang, H. Lv, S. Fang, Z. Wang, Z. Deng, X. Wang, P. Liu, W. Guo, B. Mao, H. Wang, T. Yao, X. Hong, S. Wei, X. Duan, J. Luo, Y. Wu, Cation-exchange induced precise regulation of single copper site triggers room-temperature oxidation of benzene, J. Am. Chem. Soc. 142 (2020) 12643–12650.
[88] H. Zhou, T.Y. Liu, X.Y. Zhao, Y.F. Zhao, H.W. Lv, S. Fang, X.Q. Wang, F.Y. Zhou, Q. Xu, J. Xu, C. Xiong, Z.G. Xue, K. Wang, W.C. Cheong, W. Xi, L. Gu, T. Yao, S.Q. Wei, X. Hong, J. Luo, Y.F. Li, Y.E. Wu, A supported nickel catalyst stabilized by a surface digging effect for efficient methane oxidation, Angew. Chem. Int. Ed. 58 (2019) 18388–18393.
[89] Y. Ma, Y. Ren, Y. Zhou, W. Liu, W. Baaziz, O. Ersen, C. Pham-Huu, M. Greiner, W. Chu, A. Wang, T. Zhang, Y. Liu, High-density and thermally stable palladium single-atom catalysts for chemoselective hydrogenations, Angew. Chem. Int. Ed. 59 (2020) 21613–21619.
[90] L. Lin, S. Yao, R. Gao, X. Liang, Q. Yu, Y. Deng, J. Liu, M. Peng, Z. Jiang, S. Li, Y.W. Li, X.D. Wen, W. Zhou, D. Ma, A highly CO-tolerant atomically dispersed Pt catalyst for chemoselective hydrogenation, Nat. Nanotechnol. 14 (2019) 354–361.
[91] S. Li, R. Cao, M. Xu, Y. Deng, L. Lin, S. Yao, X. Liang, M. Peng, Z. Gao, Y. Ge, J.X. Liu, W.X. Li, W. Zhou, D. Ma, Atomically dispersed Ir/α-MoC catalyst with high metal loading and thermal stability for water-promoted hydrogenation reaction, Natl. Sci. Rev. 9 (2022) nwab026.
[92] L. Lin, W. Zhou, R. Gao, S. Yao, X. Zhang, W. Xu, S. Zheng, Z. Jiang, Q. Yu, Y.W. Li, C. Shi, X.D. Wen, D. Ma, Low-temperature hydrogen production from water and methanol using Pt/α-MoC catalysts, Nature 544 (2017) 80–83.
[93] Y. Ge, X. Qin, A. Li, Y. Deng, L. Lin, M. Zhang, Q. Yu, S. Li, M. Peng, Y. Xu, X. Zhao, M. Xu, W. Zhou, S. Yao, D. Ma, Maximizing the synergistic effect of CoNi catalyst on α-MoC for robust hydrogen production, J. Am. Chem. Soc. 143 (2021) 628–633.
[94] M. Moliner, J.E. Gabay, C.E. Kliewer, R.T. Carr, J. Guzman, G.L. Casty, P. Serna, A. Corma, Reversible transformation of Pt nanoparticles into single atoms inside high-silica chabazite zeolite, J. Am. Chem. Soc. 138 (2016) 15743–15750.
[95] S. Zhang, Y. Li, C. Ding, Y. Niu, Y. Zhang, B. Yang, G. Li, J. Wang, Z. Ma, L.J. Yu, Atomic dispersion of Pt clusters encapsulated within ZSM-5 depending on aluminum sites and calcination temperature, Small Struct 4 (2022) 2200115.
[96] F.F. Tao, P.A. Crozier, Atomic-scale observations of catalyst structures under reaction conditions and during catalysis, Chem. Rev. 116 (2016) 3487–3539.
[97] W. Yuan, B. Zhu, K. Fang, X.Y. Li, T.W. Hansen, Y. Ou, H. Yang, J.B. Wagner, Y. Gao, Y. Wang, Z. Zhang, In situ manipulation of the active Au-TiO_2 interface with atomic precision during CO oxidation, Science 371 (2021) 517.
[98] W. Yuan, H. Wu, H. Li, Z. Dai, Z. Zhang, C. Sun, Y. Wang, In situ STEM determination of the atomic structure and reconstruction mechanism of the TiO_2 (001) (1×4) surface, Chem. Mater. 29 (2017) 3189–3194.
[99] W. Xi, K. Wang, Y. Shen, M. Ge, Z. Deng, Y. Zhao, Q. Cao, Y. Ding, G. Hu, J. Luo, Dynamic co-catalysis of Au single atoms and nanoporous Au for methane pyrolysis, Nat. Commun. 11 (2020) 1919.
[100] X. An, T. Wei, P. Ding, L.-M. Liu, L. Xiong, J. Tang, J. Ma, F. Wang, H. Liu, J. Qu, Sodium-directed photon-induced assembly strategy for preparing multisite catalysts with high atomic utilization efficiency, J. Am. Chem. Soc. 145 (2023) 1759–1768.
[101] H.B. Zhang, G.G. Liu, L. Shi, J.H. Ye, Single-atom catalysts: Emerging multifunctional materials in heterogeneous catalysis, Adv. Energy Mater. 8 (2018) 1701343.
[102] J. Wu, S. Helveg, S. Ullmann, Z. Peng, A.T. Bell, Growth of encapsulating carbon on supported Pt nanoparticles studied by in situ TEM, J. Catal. 338 (2016) 295–304.

[103] F. Yang, X. Wang, D. Zhang, J. Yang, D. Luo, Z. Xu, J. Wei, J.Q. Wang, Z. Xu, F. Peng, X. Li, R. Li, Y. Li, M. Li, X. Bai, F. Ding, Y. Li, Chirality-specific growth of single-walled carbon nanotubes on solid alloy catalysts, Nature 510 (2014) 522–524.
[104] F. Yang, H. Zhao, W. Wang, Q. Liu, X. Liu, Y. Hu, X. Zhang, S. Zhu, D. He, Y. Xu, J. He, R. Wang, Y. Li, Carbon-involved near-surface evolution of cobalt nanocatalysts: An in situ study, CCS Chemistry 3 (2021) 154–167.
[105] F. Yang, H. Zhao, X. Wang, X. Liu, Q. Liu, X. Liu, C. Jin, R. Wang, Y. Li, Atomic scale stability of tungsten–cobalt intermetallic nanocrystals in reactive environment at high temperature, J. Am. Chem. Soc. 141 (2019) 5871–5879.
[106] L.L. Patera, F. Bianchini, C. Africh, C. Dri, G. Soldano, M.M. Mariscal, M. Peressi, G. Comelli, Real-time imaging of adatom-promoted graphene growth on nickel, Science 359 (2018) 1243–1246.
[107] H.L. Tierney, A.E. Baber, J.R. Kitchin, E.C.H. Sykes, Hydrogen dissociation and spillover on individual isolated palladium atoms, Phys. Rev. Lett. 103 (2009) 246102.
[108] F.R. Lucci, J.L. Liu, M.D. Marcinkowski, M. Yang, L.F. Allard, M. Flytzani-Stephanopoulos, E.C.H. Sykes, Selective hydrogenation of 1,3-butadiene on platinum-copper alloys at the single-atom limit, Nat. Commun. 6 (2015) 8550.
[109] L.Z. Li, S.L. Xu, S.C. Shen, L. Wang, M. Zuo, P. Chen, H.W. Liang, A sulfur-fixing strategy toward carbon-supported Ru-based bimetallic nanocluster catalysts, Chemnanomat 6 (2020) 969–975.
[110] P. Yin, M.X. Chen, M. Zuo, L.L. Zhang, H.W. Liang, Synthesis of sub-4nm Rh-based intermetallic catalyst libraries by sulfur-anchoring strategy, ACS Mater. Lett. (2022) 1350–1357.
[111] H.L. Tierney, A.E. Baber, E.C.H. Sykes, Atomic-scale imaging and electronic structure determination of catalytic sites on Pd/Cu near surface alloys, J. Phys. Chem. C 113 (2009) 7246–7250.
[112] G.X. Pei, X.Y. Liu, X. Yang, L. Zhang, A. Wang, L. Li, H. Wang, X. Wang, T. Zhang, Performance of Cu-alloyed Pd single-atom catalyst for semihydrogenation of acetylene under simulated front-end conditions, ACS Catal. 7 (2017) 1491–1500.
[113] J. Liu, J. Shan, F.R. Lucci, S. Cao, E.C.H. Sykes, M. Flytzani-Stephanopoulos, Palladium-gold single atom alloy catalysts for liquid phase selective hydrogenation of 1-hexyne, Catal. Sci. Technol. 7 (2017) 4276–4284.
[114] C.M. Kruppe, J.D. Krooswyk, M. Trenary, Selective hydrogenation of acetylene to ethylene in the presence of a carbonaceous surface layer on a Pd/Cu(111) single-atom alloy, ACS Catal. 7 (2017) 8042–8049.
[115] F.R. Lucci, M.T. Darby, M.F.G. Mattera, C.J. Ivimey, A.J. Therrien, A. Michaelides, M. Stamatakis, E.C.H. Sykes, Controlling hydrogen activation, spillover, and desorption with Pd-Au single-atom alloys, J. Phys. Chem. Lett. 7 (2016) 480–485.
[116] G.X. Pei, X.Y. Liu, A. Wang, A.F. Lee, M.A. Isaacs, L. Li, X. Pan, X. Yang, X. Wang, Z. Tai, K. Wilson, T. Zhang, Ag alloyed Pd single-atom catalysts for efficient selective hydrogenation of acetylene to ethylene in excess ethylene, ACS Catal. 5 (2015) 3717–3725.
[117] P. Aich, H. Wei, B. Basan, A.J. Kropf, N.M. Schweitzer, C.L. Marshall, J.T. Miller, R. Meyer, Single-atom alloy Pd-Ag catalyst for selective hydrogenation of acrolein, J. Phys. Chem. C 119 (2015) 18140–18148.
[118] G.X. Pei, X.Y. Liu, A. Wang, L. Li, Y. Huang, T. Zhang, J.W. Lee, B.W.L. Jang, C.-Y. Mou, Promotional effect of Pd single atoms on Au nanoparticles supported on silica for the selective hydrogenation of acetylene in excess ethylene, New J. Chem. 38 (2014) 2043–2051.
[119] Q. Fu, Y. Luo, Catalytic activity of single transition-metal atom doped in Cu(111) surface for heterogeneous hydrogenation, J. Phys. Chem. C 117 (2013) 14618–14624.
[120] R.T. Hannagan, G. Giannakakis, R. Réocreux, J. Schumann, J. Finzel, Y. Wang, A. Michaelides, P. Deshlahra, P. Christopher, M. Flytzani-Stephanopoulos, M. Stamatakis, E.C.H. Sykes, First-principles design of a single-atom–alloy propane dehydrogenation catalyst, Science 372 (2021) 1444.
[121] L. Yang, D. Cheng, X. Zeng, X. Wan, J. Shui, Z. Xiang, D. Cao, Unveiling the high--activity origin of single-atom iron catalysts for oxygen reduction reaction, Proc. Natl. Acad. Sci. U.S.A. 115 (2018) 6626–6631.
[122] Y. Xiong, J. Dong, Z.Q. Huang, P. Xin, W. Chen, Y. Wang, Z. Li, Z. Jin, W. Xing, Z. Zhuang, J. Ye, X. Wei, R. Cao, L. Gu, S. Sun, L. Zhuang, X. Chen, H. Yang, C. Chen, Q. Peng, C.R. Chang, D. Wang, Y. Li, Single-atom Rh/N-doped carbon electrocatalyst for formic acid oxidation, Nat. Nanotechnol. 15 (2020) 390–397.
[123] H.M. Sun, Q.N. Liu, Z.Y. Gao, L. Geng, Y.S. Li, F.Y. Zhang, J.T. Yan, Y.F. Gao, K. Suenaga, L.Q. Zhang, Y.F. Tang, J.Y. Huang, In situ TEM visualization of single atom catalysis in solid-state Na-O_2 nanobatteries, J. Mater. Chem. A 10 (2022) 6096–6106.
[124] F.D. Speck, M.T.Y. Paul, F. Ruiz-Zepeda, M. Gatalo, H. Kim, H.C. Kwon, K.J.J. Mayrhofer, M. Choi, C.H. Choi, N. Hodnik, S. Cherevko, Atomistic insights into the stability of Pt single-atom electrocatalysts, J. Am. Chem. Soc. 142 (2020) 15496–15504.
[125] C.L. Yang, L.N. Wang, P. Yin, J. Liu, M.X. Chen, Q.Q. Yan, Z.S. Wang, S.L. Xu, S.Q. Chu, C. Cui, H. Ju, J. Zhu, Y. Lin, J. Shui, H.W. Liang, Sulfur-anchoring synthesis of platinum intermetallic nanoparticle catalysts for fuel cells, Science 374 (2021) 459–464.
[126] P. Yin, X. Luo, Y. Ma, S.Q. Chu, S. Chen, X. Zheng, J. Lu, X.J. Wu, H.W. Liang, Sulfur stabilizing metal nanoclusters on carbon at high temperatures, Nat. Commun. 12 (2021) 3135.